JOURNAL OF AGRICULTURAL AND FOOD CHEMISTRY
ARTICLE

J. Agric. Food Chem. 2009, 57, 6129–6139 6129
DOI:10.1021/jf9011399

A Novel Immunomodulatory Protein from *Poria cocos* Induces Toll-like Receptor 4-Dependent Activation within Mouse Peritoneal Macrophages

Hui-Hsin Chang,[†] Chen-Hao Yeh,[†] and Fuu Sheu*,[†,‡]

[†]Department of Horticulture and [‡]Research Center of Food and Biomolecules, National Taiwan University, No. 1, Sec. 4, Roosevelt Road, Taipei 10673, Taiwan, Republic of China

Poria cocos is an important Oriental medical fungus with multiple functionalities, yet its bioactive substances and the mechanisms involved have not been fully characterized. A novel immunomodulatory protein (*P. cocos* immunomodulatory protein; PCP) was purified from the dried sclerotium of *P. cocos* (Schw.) Wolf using DE-52 cellulose and gel filtration chromatography. Chromatography and electrophoresis results indicated that the native PCP (35.6 kDa) is a disulfide-linked heterodimeric glycoprotein consisting of 14.3 and 21.3 kDa subunits with N- and O-glycosylation. PCP was capable of stimulating RAW 264.7 macrophages in vitro through the induction of tumor necrosis factor-alpha (TNF-α) and interleukin-1 beta (IL-1β) as well as the regulation of nuclear factor-kappa B (NF-κB)-related gene expression. In primary mouse macrophages, PCP directly activated peritoneal cavity macrophages to induce Toll-like receptor 4 (TLR4)-mediated myeloid differentiation factor 88 (MyD88)-dependent signaling. This study demonstrated the cell surface interactions of PCP with TLR4 and the capacity of PCP for TLR4 tyrosine phosphorylation. Results obtained with peritoneal macrophages from TLR4-deficient C57BL/10ScN mice revealed that PCP-induced activation and PCP cell surface binding were significantly attenuated. Moreover, enzymatic deglycosylation decreased PCP-mediated responses, indicating that the glycosylated portion of PCP was a key factor in PCP signaling through TLR4 in peritoneal macrophages. These findings suggest that PCP is a new potential immune stimulator within *P. cocos* and that TLR4 is primarily responsible for PCP signaling in murine macrophages.

KEYWORDS: Immunomodulatory protein; *Poria cocos*; macrophage activation; TLR4; glycosylation

INTRODUCTION

Edible mushrooms have been well-characterized as valuable foods that are good sources of various nutrients including all essential amino acids, vitamins, minerals, and fibers (*1*). On the basis of their high nutrition values, some mushroom subspecies have a long history of use in medicinal purposes and display profound health-promoting benefits. Numerous mushroom compounds have been classified as possessing potential effects on the immune system, such as polysaccharides (mostly α- and β-glucans), terpenoids, proteoglycans, proteins, and various small molecular mass constituents (*2*). Among these bioactive substances, various protein-derived compounds isolated from mycelia and fruiting bodies of mushrooms enhance innate and cell-mediated immune responses and exhibit antitumor activities through host immune response activation (*3*, *4*). The activities of some mushroom polysaccharide-bound proteins are impaired by a lack of glycosylation, which regulates their signal recognition (*5*). Therefore, the structural and physicochemical properties are major factors affecting the biological activities of mushroom immunomodulators (*6*).

The sclerotium of *Poria cocos* (Schw.) Wolf, which has long been used as a sedative and diuretic, is a traditional Oriental herb mainly composed of polysaccharides, proteins, and triterpenoids. Recently, the biological activities of *P. cocos* derivatives have attracted attention in the fields of biochemistry and pharmacology. The *P. cocos*-derived extract was found to have beneficial effects on immune function (*7*, *8*). Accumulating research has indicated that certain compounds of *P. cocos* sclerotium are involved in the medicinal properties of *P. cocos*, such as its triterpene, lanostane, and polysaccharide derivatives (*6*, *9*). Nevertheless, the effective component of *P. cocos* and its molecular mechanism involved in immune modulation have not been clearly defined.

Macrophages play important roles in host defense against bacterial infections and tumor cells involved in tumor lysis and growth inhibition (*10*). In response to activating agents such as interferon (IFN)-γ, lipopolysaccharide (LPS), or some microbial products, macrophages release TNF-α, IL-1, IL-6, and nitric oxide to induce tumoricidal activity (*11*, *12*). In mammalian cells, Toll-like receptors (TLRs) play essential roles in macrophages in recognizing microbial components with subsequent immune

*Address correspondence to this author at the Research Center of Food and Biomolecules, National Taiwan University, No. 1, Sec. 4, Roosevelt Rd., Taipei 10673, Taiwan, ROC (telephone + 886 2 33664846; fax + 886 2 23673103; e-mail fsheu@ntu.edu.tw).

Published on Web 06/23/2009

responses (*13*). Of the 11 TLRs discovered so far, TLR4 is a transmembrane receptor for LPS, a component of Gram-negative bacteria (*14*), whereas TLR2 recognizes lipoteichoic acid, lipopeptides, and peptidoglycan from Gram-positive bacteria and mycobacteria (*15*, *16*). TLRs initiate serial kinase phosphorylation and subsequent NF-κB activation through interacting with MyD88 in association with TNF receptor-associated factor 6 (TRAF6) (*13*). Several studies have demonstrated a crucial involvement of TLRs in recognizing bioactive compounds derived from fungi such as β-glucans that display various biological activities via TLR-mediated signal pathways (*17*, *18*).

P. cocos is a representative mushroom used for both medical and food applications. However, the immune-stimulating compounds of *P. cocos* have not yet been fully characterized and well documented. In the present work, we isolated a novel immunomodulatory glycoprotein (*P. cocos* immunomodulatory protein; PCP) from the dried sclerotium of *P. cocos*, which has the ability to activate macrophages. We demonstrated that PCP-induced signaling is mediated through TLR4 as a candidate receptor in macrophage activation. Furthermore, the biochemical characteristics of PCP, especially its glycosylation, were examined to verify the involvement of glycosylated sites in PCP signaling, particularly in relation to its interactions with macrophages.

MATERIALS AND METHODS

Animal Experiments. C57BL/6J mice between 6 and 8 weeks old as wild-type (WT) controls were obtained from the Animal Center of National Taiwan University, Taipei, Taiwan. TLR2-deficient ($TLR2^{-/-}$, strain B6.129-$Tlr2^{tm1Kir/J}$) and TLR4-deficient ($TLR4^{-/-}$, strain C57BL/10ScN) mice from Jackson Laboratory (Bar Harbor, ME) were maintained in our animal facility under pathogen-free conditions. All animal studies were carried out according to the Institutional Animal Care and Use Committee of National Taiwan University. LPS from *Escherichia coli* and Pam3CSK4 (respective TLR4 and TLR2 agonists) were purchased from Sigma Chemical (St. Louis, MO). All other chemicals were commercially available products of analytical grade.

In our experiments, an application of laboratory-produced mouse anti-PCP monoclonal antibodies was an effective contribution to the study of characteristics of PCP. Briefly, BALB/c mice were immunized by monthly intraperitoneal injections of 50 μg of purified PCP (immunogen), which was mixed with an appropriate volume of aluminum potassium sulfate (10% w/v). Splenocytes from immunized mice were fused 3 days after an intraperitoneal injection of immunogen with mouse X63Ag8.653 myeloma cells from the American Type Culture Collection (ATCC; Manassas, VA) using 50% polyethylene glycol 1500 (Roche, Mannheim, Germany). Hybridomas were selected in a hypoxanthine−aminopterin−thymidine medium (Gibco/BRL Life Technologies, Eggenstein, Germany), and supernatants were screened by conventional immunoenzymatic assays using purified PCP as a tracer. Cells from positive wells were cloned twice by limiting dilution. Monoclonal antibodies were purified from ascites fluid from hybridoma-injected mice by protein G affinity chromatography (Amersham Biosciences, Uppsala, Sweden) according to the manufacturer's instructions.

Cell Cultures. The murine macrophage cell line RAW 264.7 was purchased from ATCC, routinely cultured in DMEM (Hyclone, Logan, UT) supplemented with 10% (v/v) FBS (Gibco/BRL Life Technologies), and maintained in a 37 °C incubator with 5% CO_2 humidified air.

Thioglycollate-elicited peritoneal macrophages were obtained from C57BL/6J, $TLR2^{-/-}$, and $TLR4^{-/-}$ mice 4 days after an intraperitoneal injection of 1.5 mL of 4% thioglycollate medium (Sigma). The cells were harvested by lavage of the peritoneal cavity with phosphate-buffered saline (PBS). Peritoneal washings were centrifuged, and the cells were resuspended in DMEM supplemented with 10% (v/v) FBS. The cell suspensions were plated onto 24-well flat-bottom plates (Costar, Cambridge, MA) and incubated for 4 h for adherence in a humidified atmosphere of 5% CO_2 at 37 °C. The nonadherent cells were removed by washing the wells with PBS. The adherent monolayer cells considered to be macrophages were further cultured.

Purification of PCP. PCP was purified from the dried sclerotium of *P. cocos* according to a previously described method (*19*) with minor modifications. The dried sclerotium was soaked in a cold 5% (v/v) acetic acid solution including 0.05 M 2-mercaptoethanol overnight and homogenized in a Waring blender following centrifugation at 8500*g* for 40 min. The ammonium sulfate was added to the crude extract up to 95% of saturation to precipitate soluble proteins in the supernatant. After the centrifugation of the extract at 10000*g* for 60 min, the precipitates were collected and then dialyzed against 10 mM Tris-HCl buffer (pH 8.2) for 72 h with at least six changes of dialysis solution. The dialysate was fractionated on a DE-cellulose (Whatman, Maidstone, U.K.) column (2.5 × 20 cm) previously equilibrated with 10 mM Tris-HCl buffer (pH 8.2). The column was eluted with a linear gradient of 0−0.5 M NaCl. The main active fractions were further purified by a fast protein liquid chromatography (FPLC) system with a Superdex 75 10/300 GL gel filtration column (Amersham Biosciences) in 50 mM phosphate buffer containing 0.15 M NaCl (pH 7.0). The resulting fraction containing PCP was dialyzed and concentrated under optimal conditions suitable for further biochemical analysis and cell culture experiments. Nevertheless, all in vitro experiments were carried out at least once in the presence of 50 μg/mL of polymyxin B (Sigma) to neutralize any undetected contamination with bacterial LPS. It was also confirmed by the *Limulus* amoebocyte lysate (LAL) clot assay (Charles River Endosafe, Charleston, MA) before use.

Molecular Weight Determination. The molecular weights of the purified and pretreated PCP were estimated by gel filtration chromatography on an FPLC-Superdex 75 column calibrated with standard proteins (Amersham Biosciences). The column was equilibrated and eluted with 50 mM phosphate buffer containing 0.15 M NaCl (pH 7.0) at a flow rate of 1 mL/min. PCP was pretreated by adding an appropriate volume of 5× sodium dodecyl sulfate (SDS) sample buffer (100 mM Tris-HCl, 4% SDS, 20% glycerol, 10% 2-mercaptoethanol, and 100 mM DTT; pH 6.8) or in the absence of reducing agents (2-mercaptoethanol and DTT). Samples were boiled for 5 min and then applied to a gel filtration column to monitor the change in molecular weight corresponding to the peak in the chromatogram. Each protein sample was analyzed by native polyacrylamide gel electrophoresis (PAGE) and SDS-PAGE on a Bio-Rad mini protein III gel apparatus (Bio-Rad Laboratories, Hercules, CA). The apparent molecular mass was determined on the basis of relative migration of protein standards (Amersham Biosciences), consisting of ovalbumin (45.0 kDa), carbonic anhydrase (30.0 kDa), trypsin inhibitor (20.1 kDa), and lysozyme (14.3 kDa). Gels were visualized by staining with Coomassie brilliant blue R250 or periodic acid−Schiff (PAS) reagent to determine the carbohydrate content.

Enzymatic Protein Deglycosylation. PCP was subjected to deglycosylation with a mixture of N- and O-linked glycosidases including PNGase F, *O*-glycosidase, α-2 (3,6,8,9) neuraminidase, β (1−4) galactosidase, and β-*N*-acetylglucosaminidase under native or denaturing conditions according to the protocols given in the enzymatic protein deglycosylation kit (Sigma). Under denaturing conditions, PCP was harvested with a buffer mixture containing 5× reaction buffer, denaturation solution, and double-distilled water. The mixture was heated at 100 °C for 5 min. Triton X-100 was then added to a final concentration of 5%. The reaction was simultaneously or individually digested with the foregoing glycosidases at 37 °C for 4 h prior to electrophoresis. In addition, PCP was treated under native conditions, incubating with all five glycosidases at 37 °C for 96 h without denaturation and Triton X-100 solution through heating.

To remove various glycosidases from the reaction mixture after digestion, the deglycosylated PCP required further electroelution under native conditions to increase its purity. Following 6% native PAGE, the deglycosylated protein band was excised from the gel and then electroeluted under non-denaturing conditions (25 mM Tris base, pH 8.3; 192 mM glycine) using an electroelution module (model 422 Electro-Eluter, Bio-Rad Laboratories) according to the manufacturer's instructions. The eluted protein was dialyzed against PBS at 4 °C and concentrated by using an Amicon concentrator (Millipore, Billerica, MA) with a 10 kDa molecular mass molecular cutoff.

Determination of TNF-α and IL-β Production. The cytokine levels of TNF-α and IL-1β were measured in cell culture supernatants by a sandwich enzyme-linked immunosorbent assay (ELISA), using OptEIA murine TNF-α and IL-1β ELISA kits (eBioscience, San Diego, CA)

according to the manufacturer's instructions, respectively. The absorbance was measured at 405 nm on a Bio-Rad 3550 microplate reader. The TNF-α or IL-1β concentrations were calculated by comparing recombinant mouse TNF-α or IL-1β as a standard.

Quantitative Real-Time Polymerase Chain Reaction (qPCR). Total RNA was extracted using the TRIzol reagent (Invitrogen, Carlsbad, CA) according to the manufacturer's instructions. The concentrations of RNAs were determined by using a NanoDrop ND-1000 spectrophotometer (NanoDrop Technologies, Wilmington, DE). The first-strand cDNA was synthesized from total RNA by using ThermoScript RT-PCR system (Invitrogen) to be utilized as a template for evaluating gene expression involved PCP immunomodulation in macrophages. Differential expression for individual genes was assessed by qPCR. Specific primer sets were designed for SYBR Green probes with Roche Probe Design Software (Roche) based on macrophage-related cytokine and immune factors sequences on NCBI. β-Actin or GAPDH (endogenous gene) was used to confirm the quality of reverse-transcripted cDNA. qPCR was performed on an Applied Biosystems 7300 Real-Time PCR System (Foster City, CA). The expression level of each target gene was quantified by the relative levels of a given mRNA according to cycling threshold (Ct) analysis.

Microarray Analysis. The Oligo GEArray Mouse NF-κB Signaling Pathway Microarray (SuperArray, Frederick, MD) was used following the manufacturer's instructions. RAW 264.7 macrophages were treated without or with PCP (100 μg/mL) or with LPS (100 ng/mL) as a positive control, and total RNA was extracted after 4 h of incubation using the TRIzol reagent. Total RNA was reverse-transcribed into the biotin-16-dUTP-labeled cRNA probe with biotin-16-uridine-5′-triphosphate (Roche) using the TrueLabeling-AMP linear RNA amplification kit according to the manufacturer's instructions. Hybridization of the biotin-labeled cRNA probe (6 μg) to the SuperArray membrane (OMM-025) was performed according to a previously described method (*20*). Images were obtained using a ChemiGenius chemiluminescence detection system (Syngene, Cambridge, U.K.) and analyzed with the Web-based GEArray Expression Analysis Suite software (SuperArray). The relative expression level of each gene was estimated by comparing its signal intensity normalized to internal control GAPDH.

Immunoprecipitation of TLR4 and Western Blotting. Immunoprecipitation assays were performed according to a previously described method (*21*) with minor modifications. Mouse peritoneal macrophages were preincubated with 100 μg of PCP for 2.5, 5, and 10 min. PCP-pretreated cells were washed in cold PBS to remove excess medium and then homogenized in ice-cold RIPA buffer containing 10 mM Tris-HCl (pH 7.4) 150 mM NaCl, 1% sodium deoxycholate, 1% Triton X-100, 0.1% SDS, 1 mM EDTA, 2 mM Na_3VO_4, 10 μg/mL leupeptin, 1 mM PMSF, and 2 mM β-glycerophosphate. After centrifugation at 10000*g* for 10 min at 4 °C, the resulting supernatants were subjected to immunoprecipitation with anti-TLR4 antibodies (eBioscience). The immunoprecipitated TLR4 proteins were subjected to Western blotting with anti-phosphotyrosine antibodies (Calbiochem, San Diego, CA). For co-immunoprecipitation, the lysate was immunoprecipitated using anti-TLR4 or laboratory-produced mouse anti-PCP monoclonal antibodies and subsequently subjected to Western blotting with either anti-PCP or anti-TLR4 antibodies (eBioscience).

Electrophoretic Mobility Shift Assay (EMSA). Nuclear protein extracts were prepared using NE-PER nuclear and cytoplasmic extraction reagents (Pierce, Rockford, IL) according to the manufacturer's instructions. A LightShift Chemiluminescent EMSA Kit (Pierce) was used to detect DNA−protein interactions. The nuclear protein extracts were incubated with double-stranded, 3′-end-biotinylated oligonucleotides encompassing the consensus NF-κB binding sequence (sense, 5′-AGTTGAGGGGACTTTCCCAGGC-3′ biotin; antisense, 5′-GCCTGGGAAAGTCCCCTCAACT-3′ biotin). A transcription factor binding analysis was performed according to a previously described method (*21*). The specificity of the identified NF-κB DNA binding activity in the nuclear extracts was confirmed by using a 200-fold molar excess of unlabeled NF-κB.

Fluorescence-Activated Cell Sorting (FACS). For surface TLR4 detection, macrophages were treated with the indicated samples for 24 h. The macrophages were stained with an unconjugated primary antibody specific for TLR4 (eBioscience) in PBS containing 2% bovine serum albumin and 0.1% sodium azide (FACS buffer) at 4 °C for 30 min. Subsequently, cells were washed twice with FACS buffer and incubated with a FITC-conjugated secondary antibody. Acquisition and analysis were performed with FACScan using CellQuest software (BD Biosciences, San Jose, CA). The results are expressed as the total mean fluorescence intensity (MFI) and percentage of positive fluorescent cells.

Macrophage Binding Study. Samples were labeled with fluorescein isothiocyanate (FITC) using an FITC protein labeling kit (Pierce) according to the manufacturer's instructions. For evaluating the binding of PCP to macrophages, cells were preincubated with 25 μg/mL of anti-TLR2, anti-TLR4, isotype-matched control mouse IgG antibodies (eBioscience), or unlabeled competitive PCP (100 μg/mL) for 30 min. After preincubation, 100 μg/mL of FITC-labeled PCP was incubated for an additional 1 h. After washing with PBS, cells were fixed with 4% paraformaldehyde in PBS and then stained with 1 μg/mL of DAPI (Sigma) before examination by fluorescent microscopy using a Nikon Eclipse E600 microscope (Nikon, Melville, NY). A macrophage-binding assay was also performed using FITC-labeled PCP as a detection antibody by flow cytometry.

Statistical Analysis. All values are presented as the mean ± SD of three independent experiments performed in triplicate. Statistical comparisons were performed by analysis of variance (ANOVA). Differences were considered to be statistically significant at p values of < 0.05 ($p < 0.05$).

RESULTS

Purification and Biochemical Characteristics of PCP. To isolate the novel bioactive protein from *P. cocos* for further identification, the crude protein from dried sclerotium of *P. cocos* obtained by homogenization and ammonium sulfate precipitation was fractionated by DE-52 cellulose anion exchange chromatography with a linear gradient of NaCl (0−0.5 M in 10 mM Tris-HCl buffer; pH 8.2). The elution profile obtained by measuring the absorbance at 280 nm gave a prominent peak (**Figure** 1**A**). Fractions of this peak were pooled to determine the stimulatory activity toward RAW 264.7 macrophages. Remarkable activity was observed in this peak due to an increase in TNF-α production in RAW 264.7 macrophages. The active fraction purified using an FPLC gel filtration column showed a single peak (**Figure** 1**B**, solid line) with a native molecular mass of 35.6 kDa based on the calibration curve generated from the standard proteins. This active fraction was designated PCP. The yield was approximately 165 mg of the purified PCP obtained from 1 kg of the dried sclerotium of *P. cocos*. Further analysis by SDS-PAGE revealed that the fraction protein yielded two bands with molecular masses of 14.3 and 21.3 kDa (**Figure** 1**C**, lane 2). Therefore, we suggest that the purified protein was a heterodimer protein consisting of 14.3 and 21.3 kDa subunits. To prove our suggestion, PCP was pretreated with SDS sample buffer in the presence or absence of reducing agents (DTT and 2-mercaptoethanol) and then subjected to fractionation on an FPLC gel filtration column to verify the molecular mass of the native and denatured forms of protein under reducing and nonreducing conditions. As shown in **Figure** 1**B**, the native PCP exhibited a single peak (solid line), whereas two distinctive peaks were observed (dotted line) after simultaneous treatments with reducing agents, detergents, and boiling. In contrast, the pretreated PCP that was boiled in SDS-containing buffer under nonreducing conditions resulted in a single peak (dashed line) by gel filtration chromatography, suggesting the presence of an intermolecular disulfide bond.

Various types of electrophoresis were further used to examine the biochemical characteristics of purified PCP. After SDS-PAGE under reducing conditions, the polyacrylamide gel stained with PAS reagent revealed that the 21.3 kDa subunit showed a positive result (**Figure** 1**C**, lane 3), indicating that PCP contained carbohydrates. Additionally, PCP appeared as a single band in the native PAGE (**Figure** 1C, lane 4), confirmed by gel filtration chromatography under native conditions. Western blotting

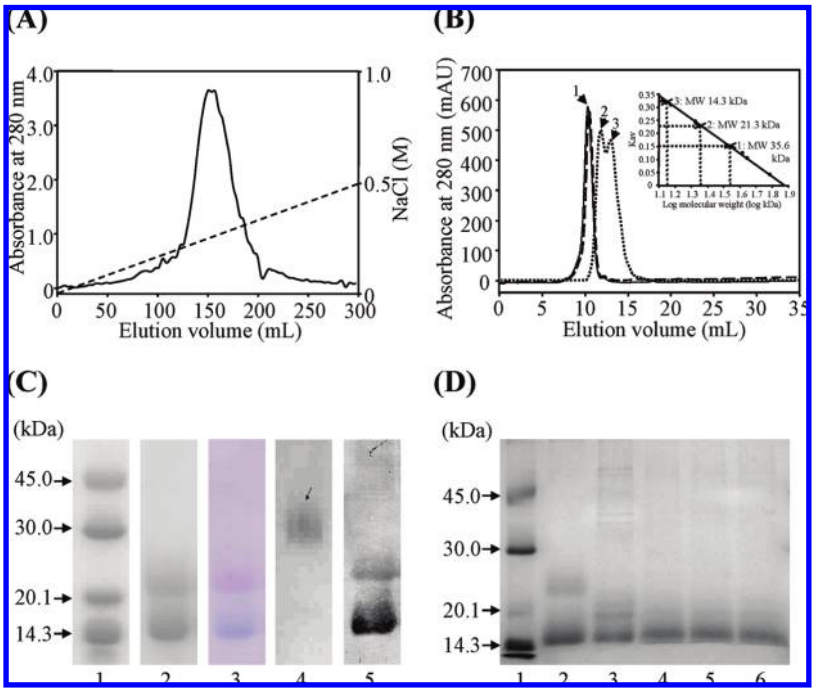

Figure 1. Purification chromatography and biochemical characteristics of PCP. (**A**) Elution profile of PCP from a DE-52 cellulose column. (**B**) Elution profile of PCP and its derived samples from an FPLC gel filtration column. Native PCP (solid line), denatured PCP (dotted line), and nonreduced PCP (dashed line) were subjected to gel filtration chromatography. The calibration curve was a plot of log molecular weight (log M_w) of protein versus ratio of the elution volume to the void volume (V_e/V_0). (**C**) PCP was identified by SDS-PAGE with Coomassie brilliant blue (lane 2) and periodic acid−Schiff (lane 3) staining: native PAGE with Coomassie brilliant blue staining (lane 4); Western blotting using monoclonal antibodies against PCP (lane 5); molecular weight markers (lane 1). (**D**) SDS-PAGE of native and deglycosylated PCP: native PCP control (lane 2); PCP deglycosylated with PNGase F under denaturing conditions (lane 3); PCP deglycosylated with PNGaseF, *O*-glycosidase, and α-2 (3,6,8,9) neuraminidase under denaturing conditions (lane 4; PCP deglycosylated with PNGaseF, *O*-glycosidase, α-2 (3,6,8,9) neuraminidase, β (1−4) galactosidase, and β-*N*-acetylglucosaminidase under denaturing conditions (lane 5); deglycosylation of PCP with all five enzymes under native conditions (lane 6); molecular weight markers (lane 1).

showed that the 14.3 and 21.3 kDa subunits of PCP were both recognized by anti-PCP monoclonal antibodies (**Figure** 1**C**, lane 5; see Supporting Information, Supplementary Figure S1). Isoelectric focusing on polyacrylamide in the pH range of 3−9 revealed a single band of PCP with a p*I* of 5.2 (see Supporting Information, Supplementary Figure S2). Furthermore, the N-terminal amino acid sequences (VTVNVADAM) and amino acid composition of the 21.3 kDa subunit were identical to those of the 14.3 kDa subunit (see Supporting Information, Supplementary Table S1), except for the carbohydrate content (due to the difference in their molecular weights). Taken together, these results suggest that PCP is an interdisulfide-linked heterodimer with a molecular mass of 35.6 kDa consisting of 14.3 and 21.3 kDa subunits.

To investigate structural aspects of the N-linked and O-linked glycans, PCP was subjected to enzymatic deglycosylation by sequential addition of each of enzyme containing PNGase F, *O*-glycosidase, α-2 (3,6,8,9) neuraminidase, β (1−4) galactosidase, and β-*N*-acetylglucosaminidase. Upon incubation of PNGase F under denaturing conditions, the electrophoretic mobility of the molecular mass of the 21.3 kDa subunit had a significant decrease (**Figure** 1**D**, lane 3). This caused the removal of all types of N-linked glycans, but still left the remains of an approximate molecular mass of 18 kDa. PCP was deglycosylated simultaneously by PNGaseF, *O*-glycosidase, and α-2 (3,6,8,9) neuraminidase, leading to the abolishment of the 21.3 kDa band. Only the 14.3 kDa band remained as the predominant component (**Figure** 1**D**, lane 4). However, there was no effect in SDS-PAGE by digestion of denaturing PCP with supplementary β (1−4) galactosidase and β-*N*-acetylglucosaminidase (**Figure** 1**D**, lane 5). For deglycosylation of PCP with all five enzymes under native conditions, a clear band shift appeared (**Figure** 1**D**, lane 6). The shift in mobility was similar to the shift observed when PCP was deglycosylated under denaturing conditions. This indicates that PCP is composed of both N- and O-linked glycans.

PCP Induces Activation of NF-κB Signaling Pathway in Mouse Macrophage RAW 264.7 Cells. To determine the immunomodulatory activities and suitable concentrations of PCP for further experiments, the dose effect of PCP on TNF-α and IL-1β secretion of mouse macrophage RAW 264.7 cells was investigated. In our preliminary experiments, we first excluded the possibility of endotoxin contamination of PCP by the LAL gel-clot and polymyxin B assay (see Supporting Information, Supplementary Table S2 and Figure S3). This dose−response study revealed that PCP possessed predominant activity of promoting TNF-α and IL-1β production by RAW 264.7 macrophages at concentrations ranging from 20 to 160 μg/mL (**Figure** 2**A**). In the presence of PCP (80 μg/mL), the amounts of TNF-α and IL-1β secreted were up to 16500 and 460 pg/mL, respectively. The maximum TNF-α and IL-1β production was observed at 160 μg/mL of PCP. Transcription factor NF-κB is widely recognized as a critical mediator of immune responses such as enhancing the expression of TNF-α (*22*). Accordingly, the stimulatory effect of PCP on macrophages was highly correlated with the activation of NF-κB. To investigate the expression profile of NF-κB-related genes in RAW 264.7 macrophages exposed to PCP alone, we performed microarray experiments using the Oligo GEArray Mouse NFκB Signaling Pathway Microarray. Of the 128 genes covered by the Oligo Microarray OMM-025, 20 genes were found to be overexpressed in the PCP-stimulated cells compared to the control cells incubated with culture medium only for the chosen filter criteria (**Figure** 2**B**). In particular, the regulated genes

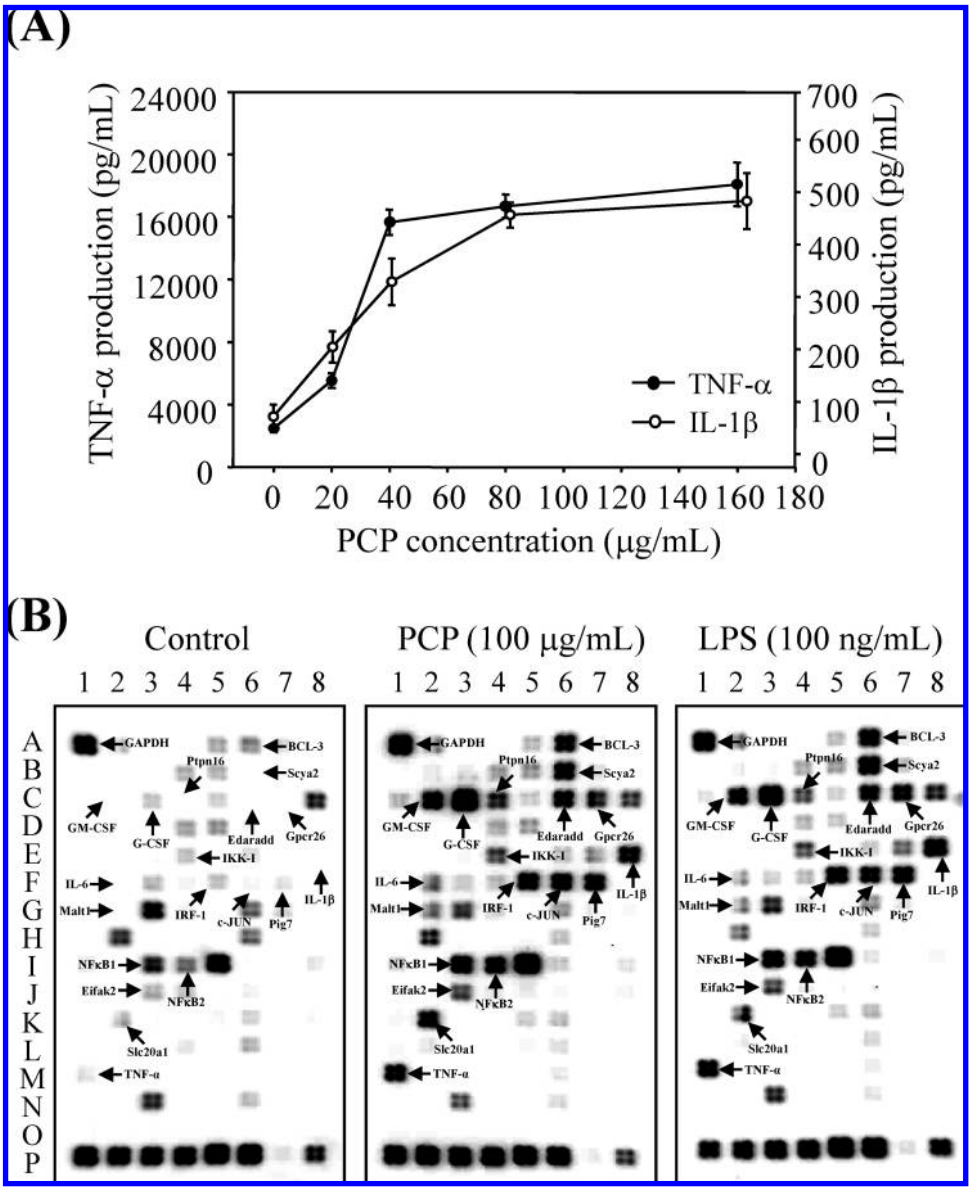

Figure 2. Effect of PCP on cytokine release and NF-κB-related gene regulation in RAW 264.7 macrophages: (**A**) dose response of PCP stimulation on TNF-α and IL-1β production by RAW 264.7 macrophages; (**B**) Mmicroarray analysis of NF-κB signaling pathway in PCP-mediated RAW 264.7 macrophage activation. Microarray analysis was performed on mRNAs extracted from RAW 264.7 macrophages pretreated with medium alone (control, left panel), 100 μg/mL of PCP (middle panel), and 100 ng/mL of LPS (right panel) as a positive control for 4 h, using cDNA array blots containing 128 genes related to NF-κB-mediated signal transduction and housekeeping genes.

(promoting cell proliferation, cell differentiation, growth factor expression, and cytokine activity) were related to members of the NF-κB pathway (**Table** 1), and similar effects were observed in the LPS-stimulated cells. These indicate that PCP is an effective activator of murine macrophages, and its molecular mechanism on macrophages is similar to LPS-mediated macrophage activation.

TLR4 Is Involved in PCP-Induced Mouse Peritoneal Macrophage Activation. Genes with relevance for the role of PCP in cytokine induction were further analyzed by qPCR. Similarly, PCP was able to enhance cytokine secretion, such as those of TNF-α and IL-1β in mouse peritoneal macrophages. As shown in **Table** 2, PCP markedly increased the gene expressions of TNF-α, iNOS, IL-1β, IL-6, IL-12, and IL-18 in time-dependent manners. The highest peak of TNF-α gene expression was observed at 2 h, and those of other cytokines appeared between 4 and 8 h, with the peak levels at 16 h after PCP treatment. In addition, gene expressions of NF-κB, MyD88, TRAF6, and Toll-IL-1 receptor domain-containing adapter protein (TIRAP) increased with PCP stimulation, and the maximal response of those was obtained within 2−4 h during the period of observation (**Figure** 3**A**). This indicated their involvement in tandem in PCP-induced macrophage activation. TLR4 expression was up-regulated on peritoneal macrophages by co-incubation with PCP, whereas the expression of TLR2 and TLR6 remained unaffected (**Figure** 3**B**). To determine the involvement of these receptors in the interaction of macrophages with PCP, peritoneal macrophages obtained from TLR2$^{-/-}$, TLR4$^{-/-}$, and WT control C57BL/6J mice were incubated with PCP, LPS as TLR4 agonist, and Pam3CSK4 as TLR2 agonist in vitro. Further investigation revealed that there was a significant elevation of TNF-α in both WT and TLR2$^{-/-}$ macrophages in response to PCP stimulation, whereas PCP-induced activities were almost absent in TLR4$^{-/-}$ macrophages (**Figure** 3**C**). A similar elevation by PCP in IL-1β

Table 1. Selection and Category of Overexpressed NF-κB-Related Genes in RAW 264.7 Macrophages Investigated by Oligo GEArray Mouse NFκB Signaling Pathway Microarray OMM-025[a,b]

category and gene name	gene symbol	GenBank accession no.	fold change (PCP-induced)	fold change (LPS-induced)
activation of the NF-κB pathway				
EDAR (ectodysplasin-A receptor)-associated death domain	Edaradd	XM_147719	3.59	3.16
inhibitor of κB kinase epsilon	IKK-I	NM_019777	1.67	1.48
mucosa associated lymphoid tissue lymphoma translocation gene 1	Malt1	NM_172833	1.92	1.60
NF-κB responsive genes				
colony-stimulating factor 2 (granulocyte-macrophage)	GM-CSF	NM_009969	4.11	3.35
colony-stimulating factor 3 (granulocyte)	G-CSF	NM_009971	4.89	4.29
interleukin 6	IL-6	NM_031168	2.14	1.61
interferon regulatory factor 1	IRF-1	NM_008390	2.77	2.48
tumor necrosis factor α	TNFα	NM_013693	2.86	2.56
other factors involved in the NF-κB pathway				
B-cell leukemia/lymphoma 3	BCL-3	NM_033601	1.95	1.93
chemokine (C−C motif) ligand 2	Scya2	NM_011333	3.62	3.83
dual specificity phosphatase 1	Ptpn16	NM_013642	2.80	2.14
endothelial differentiation, lysophosphatidic acid G-protein-coupled receptor, 2	Gpcr26	NM_010336	2.92	3.19
interleukin 1 α	IL-1α	NM_010554	1.81	2.10
interleukin 1 β	IL-1β	NM_008361	3.23	3.63
Jun oncogene	c-JUN	NM_010591	3.32	2.76
LPS-induced TN factor	Pig7	NM_019980	2.98	2.93
ubiquitin-conjugating enzyme E2D 3 (UBC4/5 homologue, yeast)	NFκB1	NM_008689	1.60	1.45
nuclear factor of κ light polypeptide gene enhancer in B-cells 2, p49/p100	NFκB2	NM_019408	1.79	1.58
protein kinase, interferon-inducible double-stranded RNA dependent	Eifak2	NM_011163	1.52	1.36
solute carrier family 20, member 1	Slc20a1	NM_015747	2.47	1.56

[a] Discrepancy between the initial signals and repeated signal = 1. [b] Multiple genes are plotted in this array, and the representative one is listed.

Table 2. Gene Expression of TNF-α, iNOS, IL-1β, IL-6, IL-12, and IL-18 in Mouse Peritoneal Macrophages from C57BL/6J Mice Exposed to PCP for Various Times[a,b]

	relative normalized mRNA expression after incubation for					
gene	0 h	2 h	4 h	8 h	16 h	24 h
TNF-α	1.00 ± 0.13	9.58 ± 0.76*	8.11 ± 0.84*	3.63 ± 0.63*	3.68 ± 0.51*	1.31 ± 0.20
iNOS	1.00 ± 0.06	0.99 ± 0.15	1.78 ± 0.52	7.26 ± 0.37*	8.28 ± 0.63*	1.99 ± 0.58
IL-1β	1.00 ± 0.19	20.97 ± 1.43*	31.78 ± 1.78*	156.50 ± 1.63*	119.43 ± 2.98*	66.72 ± 1.03*
IL-6	1.00 ± 0.17	7.16 ± 0.66*	14.72 ± 1.22*	13.09 ± 0.82*	11.00 ± 1.64*	2.54 ± 0.33
IL-12	1.00 ± 0.22	8.00 ± 0.77*	8.88 ± 0.98*	44.32 ± 0.55*	16.91 ± 1.87*	2.28 ± 0.76
IL-18	1.00 ± 0.17	0.98 ± 0.23	1.55 ± 0.32	1.70 ± 0.43	4.38 ± 0.66*	1.01 ± 0.54

[a] mRNA expression levels were normalized to β-actin mRNA levels. [b] Data are expressed as fold change relative to the untreated control (0 h) and represent the means ± SD of three independent experiments (*, $p < 0.05$).

production was observed in the cells of WT and TLR2$^{-/-}$ mice but not TLR4$^{-/-}$ mice (see Supporting Information, Supplementary Figure S4). NF-κB activation plays a crucial role in cellular responses to stimuli such as LPS (*23*). Therefore, we investigated whether PCP employed a similar activation pathway by monitoring its ability to activate NF-κB translocation into the nucleus using EMSA. As shown in **Figure 3D**, PCP at concentrations ranging from 50 to 150 μg/mL was able to induce NF-κB DNA-binding activities of WT macrophages (upper panel, lanes 2−4) as well as LPS and Pam3CSK4 stimulation (lanes 5 and 6). Conversely, TLR4$^{-/-}$ macrophages displayed impaired NF-κB activation under PCP and LPS treatment but not with the Pam3CSK4 control (lower panel, lanes 2−6). These results indicate that PCP may induce activation of the NF-κB signaling pathway, which is mediated through TLR4 in murine macrophages.

PCP Interacts with TLR4 in Mouse Peritoneal Macrophages. To further study the interaction between TLRs and PCP, the binding of PCP to the cell surface of peritoneal macrophages was demonstrated by comparing the FACS analysis and fluorescence microscopy results of TLR4$^{-/-}$ and WT control mice. Furthermore, we also examined the effects of anti-TLR2 and anti-TLR4 antibodies on PCP cell surface binding in mouse peritoneal macrophage cultures in a fluorescence microscopy experiment. The FACS analysis indicated that PCP bound to the cell surface of WT macrophages as demonstrated by a clear shift in fluorescence intensity (**Figure 4A**, left panel). However, diminished levels of PCP binding were observed with TLR4$^{-/-}$ cells (**Figure 4A**, right panel). The similarity in fluorescence microscopic results showed that cell surface binding of PCP was observed in WT macrophages incubated with FITC-labeled PCP, which did not bind to the surface of TLR4$^{-/-}$ macrophages (**Figure 4B**). Pretreatment with anti-TLR2 antibodies or control IgG had no significant effect. Nevertheless, anti-TLR4 antibodies markedly reduced PCP cell surface binding, confirming the physical interaction of PCP with TLR4 in mouse peritoneal macrophages. The result also indicated that excess nonfluorescent unlabeled PCP was shown to compete for cell surface PCP binding sites, resulting in a significant decrease in the green fluorescence (**Figure 4B**). We further utilized immunoprecipitation and immunoblotting methods to investigate cell surface interactions of PCP with TLR4. As shown in **Figure 4C**, mutual coprecipitation with both TLR4 and PCP showed that there was an interaction between PCP and TLR4, respectively. It has been reported that LPS-stimulated

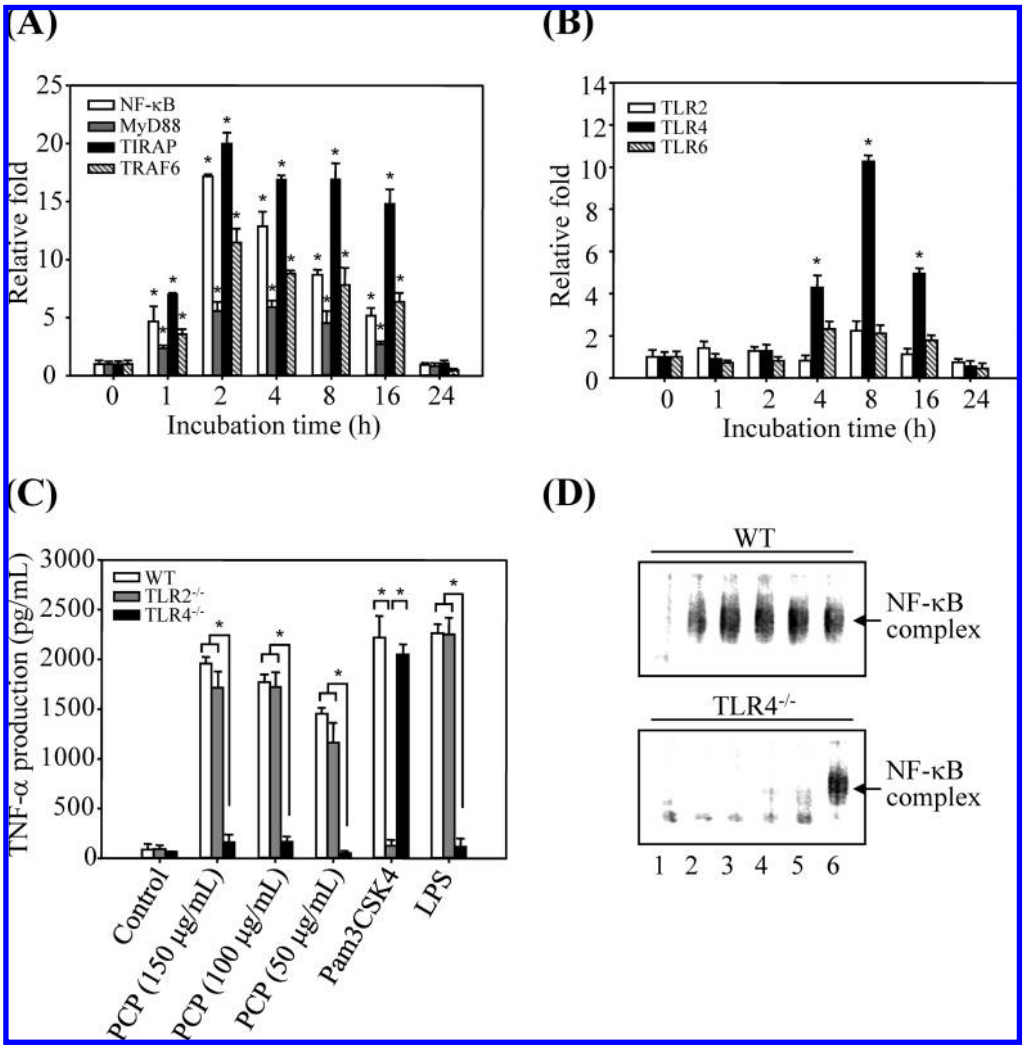

Figure 3. Involvement of TLR4 in PCP-induced activation of mouse peritoneal macrophages. Total RNA was extracted from the cells treated with 100 μg/mL of PCP in a time-dependent manner and subjected to RT-PCR using the corresponding primers of NF-κB, MyD88, TIRAP, and TRAF6 (**A**) and TLR2, TLR4, and TLR6 (**B**), through detection by quantitative real-time PCR. The mRNA levels are given as the mean $\pm$ SD normalized to β-actin levels for each sample. $*$, $p < 0.05$ compared to the culture medium control (0 h). (**C**) Effect of PCP on TNF-α induction by mouse peritoneal macrophages from C57BL/6J (WT) and TLR-deficient (TLR2$^{-/-}$ and TLR4$^{-/-}$) mice. The cells were incubated with medium alone (control), PCP (50, 100, 150 μg/mL), Pam3CSK4 (100 ng/mL), and LPS (1 μg/mL) for 20 h, and then their TNF-α levels in culture supernatants were determined. $*$, $p < 0.05$ among the different groups. (**D**) WT and TLR4$^{-/-}$ macrophages were treated with medium alone (lane 1), PCP (50, 100, 150 μg/mL, lanes 2−4), LPS (1 μg/mL, lane 5), and Pam3CSK4 (100 ng/mL, lane 6) for 2 h. NF-κB activity was determined by EMSA after the binding of nuclear proteins to consensus oligonucleotide corresponds to the NF-κB binding site.

tyrosine phosphorylation of TLR4 is involved in downstream signaling events induced by LPS (*23*). In the present study, PCP was demonstrated to stimulate TLR4 tyrosine phosphorylation in a time-dependent manner (**Figure** 4**D**).

Glycosylation of PCP Is the Key Factor in PCP Signaling through TLR4 within Murine Macrophages. To investigate whether the polysaccharide moiety of PCP was critical for its immunomodulatory activity, we compared the capability of glycosylated and nonglycosylated fractions of PCP using enzymatic deglycosylation and electroelution under native conditions on macrophage activation. Meanwhile, it was verified that the ability of PCP in inducing macrophage activation did not decrease after electroelution under native conditions as demonstrated by the enhancement of TNF-α and IL-1β production by mouse peritoneal macrophages (see Supporting Information, Supplementary Figure S5). Flow cytometry analysis revealed that PCP bound to the cell surface of peritoneal macrophages obtained from WT and TLR2$^{-/-}$ mice, whereas there was a significant reduction in PCP cell surface binding on TLR4$^{-/-}$ macrophages (**Figure** 5**A**, left panel). Removal of oligosaccharide side chains from PCP caused significant loss of cell-binding activity on WT and TLR2$^{-/-}$ macrophages (**Figure** 5**A**, right panel). Similarly, the ability of the glycosylated fraction to enhance macrophage cytokine secretion (TNF-α and IL-1β) was superior to that of the nonglycosylated fraction (**Figure** 5**B**). Our results also showed that the native PCP (glycosylated fraction) was able to increase the cell surface expression of TLR4 in peritoneal macrophages from WT mice, but not that of deglycosylated PCP or LPS as the negative control (*24*) (**Figure** 5**C**). These results indicated that PCP-induced macrophage activation was directly correlated with the polysaccharide moiety of PCP.

DISCUSSION

This paper is the first study to reveal that PCP, a novel immunomodulatory protein from *P. cocos*, is an effective activator of murine macrophages. Our characterization study indicates that PCP is a disulfide-linked heterodimeric glycoprotein with a molecular mass of 35.6 kDa consisting of two subunits (of

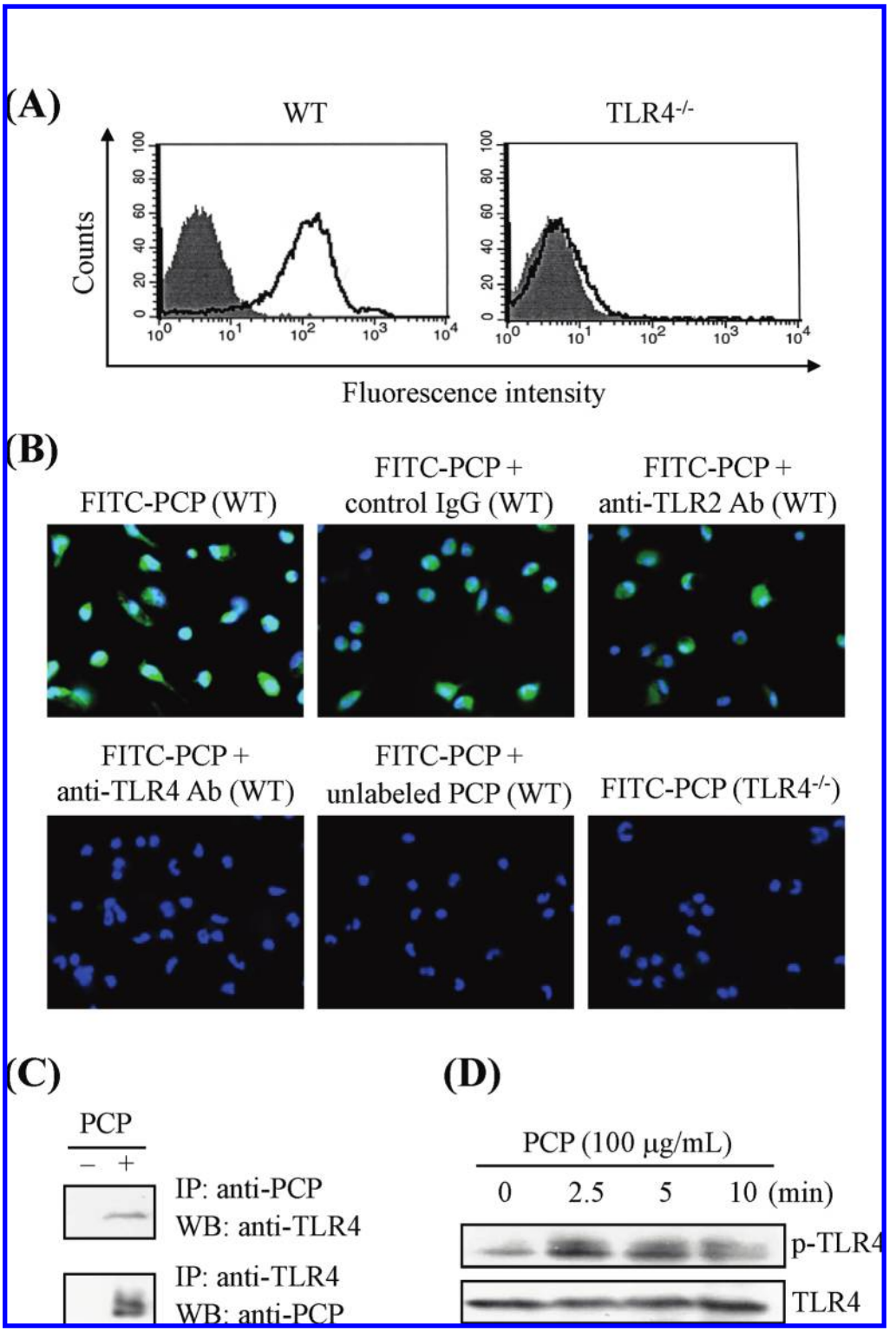

Figure 4. Characterization of PCP cell surface binding to TLR4. (**A**) Peritoneal macrophages obtained from WT and TLR4$^{-/-}$ mice were unstained (shaded area) or stained with FITC-labeled PCP (solid line) for 30 min. The cells were then analyzed by flow cytometry for the cell surface binding ability of PCP. (**B**) WT and TLR4$^{-/-}$ macrophages were preincubated with neutralizing antibodies as indicated or unlabeled competitive PCP. Cells were incubated with FITC-labeled PCP (100 μg/mL; green fluorescence) and subsequently stained with DAPI (1 μg/mL; blue fluorescence) for visualizing by fluorescence microscopy. Results shown are representative of three independent experiments. Magnification, $\times$400. (**C**) WT macrophages were incubated with PCP (100 μg/mL) or medium alone for 30 min and then lysed. Cell lysates were precipitated with anti-PCP (upper panel) or anti-TLR4 (lower panel) antibodies. Blots were immunoprobed with anti-TLR4 (upper panel) or anti-PCP (lower panel) antibodies. (**D**) Time course of TLR4 protein phosphorylation mediated by PCP. Cell lysates from control or PCP-treated macrophages at the indicated times were immunoprecipitated with anti-TLR4 antibodies and then resolved by SDS-PAGE. Blots were probed with antiphosphotyrosine (upper panel) or anti-TLR4 (lower panel) antibodies.

14.3 and 21.3 kDa). Furthermore, PCP is an N- and O-glycosylated protein that has approximately 7 kDa of its molecular mass contributed by carbohydrates. Among the active ingredients found in medicinal mushrooms, certain fungal glycoproteins

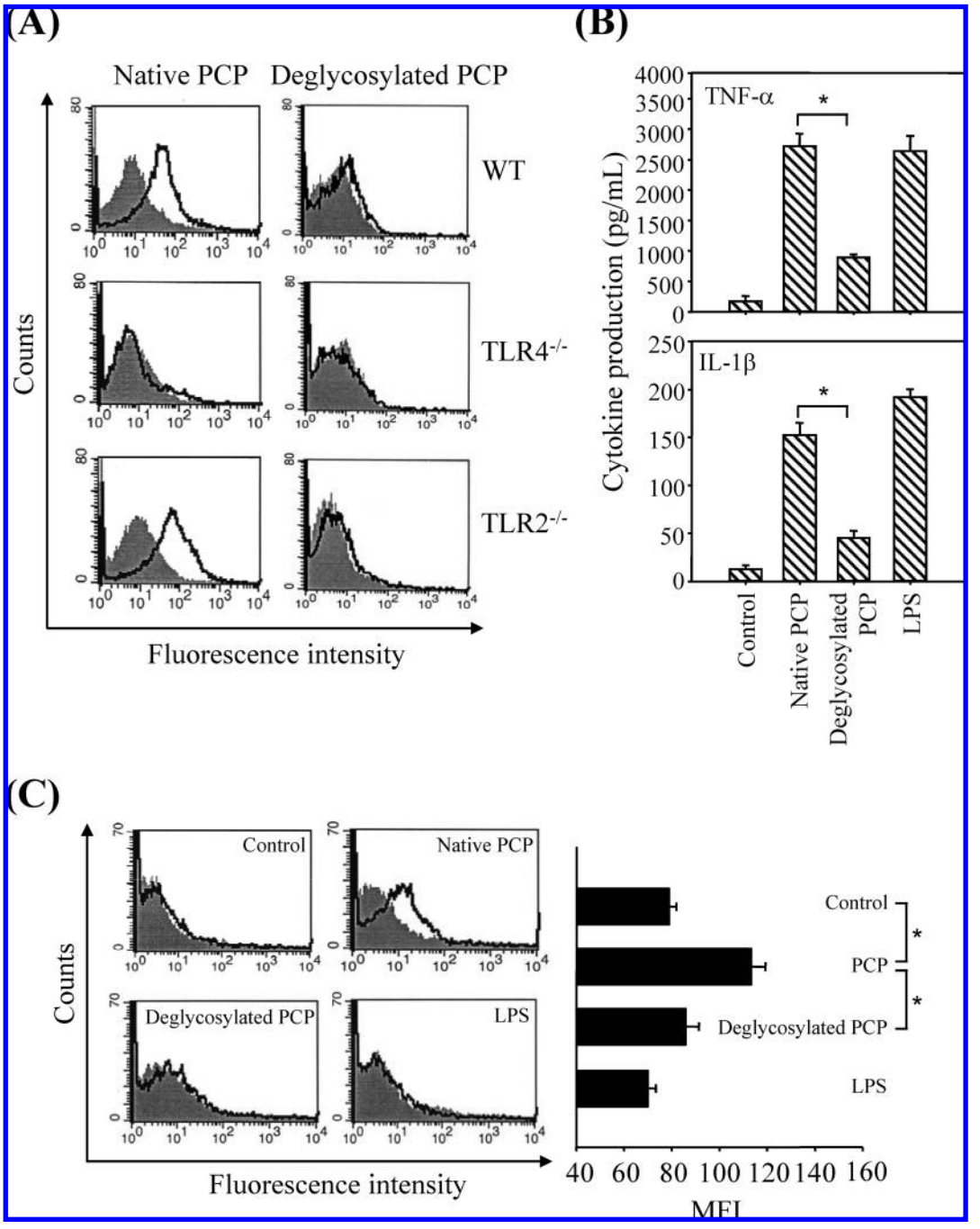

Figure 5. Effect of glycosylation of PCP on PCP-induced macrophage activation. (**A**) Peritoneal macrophages from WT, TLR4$^{-/-}$, and TLR2$^{-/-}$ mice were unstained (shaded area) or stained with different FITC-labeled samples (solid line) for 30 min and then analyzed by flow cytometry. (**B**) WT macrophages were incubated with the indicated stimulants (100 μg/mL, respectively) for 20 h. The supernatants were collected to determine their TNF-α (upper panel) and IL-1β (lower panel) levels. $*$, $p < 0.05$ compared to the control. (**C**) WT macrophages were incubated with 100 μg/mL of native or deglycosylated PCP, and LPS (1 μg/mL) for 20 h, followed by flow cytometry analysis. The shaded area shows FITC-conjugated secondary antibody control staining. The solid line indicates the cell surface expression of TLR4 on macrophages. The histograms were quantified and represented as mean fluorescence intensity (MFI).

have been isolated to possess beneficial effects in modulating the immune system and in inhibiting tumor growth (*25*, *26*). Fungal immunomodulatory protein classes (FIPs) were identified in *Ganoderma lucidium*, *Flammulina velutipes*, *Volvariella volvacea*, and *Ganoderma tsugae* and designated LZ-8, FIP-*fve*, FIP-*vvo*, and FIP-*gts*, respectively (*19*, *27*−*29*). FIPs have been shown to share high homology in amino acid sequences and exhibit hemagglutination activity (*19*). PCP was not classified as a lectin or FIP family due to its incapacity to aggregate mouse red blood cells (see Supporting Information, Supplementary Figure S6). Lack of hemagglutination activity is helpful in the therapeutic development of PCP. In addition, PCP is composed of significant amounts of half-cysteine, histidine, and methionine (see Supporting Information, Supplementary Table S1). In contrast, these amino acids were not detected in FIPs (*19*). Therefore, we found a new immunomodulatory protein, PCP, which was not identical to any known protein derived from *P. cocos* or from other medicinal mushrooms.

The immunomodulatory activity of PCP was initially explored by examining the induction of TNF-α and IL-1β production by stimulated RAW 264.7 macrophages. It is well-known that NF-κB related cascades are the major signaling pathway involved

in macrophage activation (*14*). On the basis of the positive results received from cytokine production, we further tested the effects of PCP on RAW 264.7 macrophages measured by the NF-κB related signaling pathway microarray. Herein, we demonstrated that PCP-induced activation of macrophages was similar to that observed with LPS stimulation. Generally, TLR4 is crucial for macrophage responses to LPS and permits inferences related to the mechanism of LPS signaling to be made (*14*). This prompted us to investigate whether TLR4 is a candidate receptor for PCP. Recent evidence indicated that TIR domain-containing adaptors (such as MyD88 and TIRAP) are involved in early activation of TLR signaling pathways (*13*). Upon stimulation, TLR recruits the IL-1R-associated kinase (IRAK) family via adaptor MyD88 followed by sequential phosphorylation and then associates with TRAF6, leading to the activation of NF-κB and mitogen-activated protein (MAP) kinases (*13*). Our results demonstrated that PCP up-regulated both MyD88 and TIRAP mRNA expression, similar to the mRNA expression of TRAF6 and NF-κB. These results indicated that MyD88-dependent NF-κB signaling is necessary for macrophage activation in response to PCP. We further demonstrated a significant increase in TLR4 mRNA expression in PCP-induced peritoneal macrophages. To verify the involvement of TLR4 on PCP-mediated macrophage activation, the PCP-induced activation of peritoneal macrophages isolated from WT, TLR2$^{-/-}$, and TLR4$^{-/-}$ mice were examined. Using in vitro binding and immunoprecipitation assays, we found a direct association of PCP and TLR4 with the induction of PCP-mediated TLR4 tyrosine phosphorylation in peritoneal macrophages. On the basis of the in vitro data, we found a strong impact of TLR4 on macrophage activation triggered by PCP, indicating that TLR4 plays a major role in PCP signaling. Furthermore, TLR4 is identified as a signaling receptor, which is physically associated with other surface molecules such as CD14 and MD2 (*24*), suggesting that these factors may contribute to the recognition of PCP by TLR4.

Antigen recognition by TLRs is critical for eliciting activation of the innate immune system and leads to the secretion of many immune mediators such as TNF-α, IL-1β, and several chemokines. Therefore, the involvement of TLRs is likely to play a considerable role in the initiation and perpetuation of the immune response. In this study, we demonstrated that PCP was able to activate murine macrophages by cytokine production and NF-κB-dependent regulation. Recently, an increasing number of studies have indicated that TLR4 recognizes several other ligands in addition to LPS, such as Taxol, host-derived molecules, and oligosaccharide fragments of hyaluronic acid and heparan sulfate (*30*−*32*). Furthermore, the involvement of TLR4 in recognizing some fungal polysaccharide complexes induces the phenotypic and functional maturation of dendritic cells and macrophages (*17*, *33*). The mannan fraction from *Candida albicans* and *Saccharomyces cerevisiae* induces TNF-α production in a manner dependent on CD14 and TLR4 (*34*). Among these TLR4 agonists, a soluble branched β-(1,4)-glucan was reported to be one of the main components recognized by TLR4 (*35*). On the basis of these viewpoints, mushroom-derived polysaccharides might have significant impacts on clinical applications by directly activating the innate immune response via TLR-mediated signaling. For these reasons, we theorized that the polysaccharide moiety of PCP might be a potent component in the triggering of the TLR4-mediated macrophage response.

To identify the components within PCP that are crucial for macrophage regulation, PCP was digested with various glycosidases to specifically remove N- and O-linked glycans under native conditions. The removal of carbohydrates from PCP resulted in abolishing the increase in TLR4 cell surface expression and TNF-α and IL-1β secretion. However, the deglycosylated PCP still displayed a slight effect on the TNF-α and IL-1β production. We inferred that the remaining activity resulted from its imperceptible carbohydrate remains after deglycosylation treatment. These findings strongly suggested that the polysaccharide moiety at the base of PCP possessed the capacity to activate a TLR4-dependent response. Protein glycosylation is the most abundant and important post-translation modification that regulates protein structure and function in eukaryotes. Wide ranges of functions were attributed to glycan structures covalently linked to asparagine residues within the asparagine−X−serine/threonine consensus sequence (Asn−Xaa−Ser/Thr) (*36*). As a 65 kDa fungus glycoprotein from *C. albicans* (MP65), it has been reported that MP65 was able to induce the cytokine response by dendritic cells due to its mannosylated moiety through TLR2 and TLR4 (*37*). Thus, the inability of MP65 devoid of the mannosylated moiety to stimulate pro-inflammatory cytokines should be greatly ascribable to its inability to bind to TLRs (*38*). This evidence supports the polysaccharide moiety of PCP being considered critical for interaction with a pattern recognition receptor, TLR4, to drive macrophage activation.

In conclusion, PCP is an immunomodulatory glycoprotein with unique features. The current study presents the first systematic investigation of PCP activating murine macrophages by a TLR4-dependent mechanism. Our results also provide valuable information regarding the polysaccharide moiety of PCP. These observations strongly support further studies of PCP and *P. cocos* to explore their overall modulatory nature toward mammalian cells and reveal their pharmaceutical potential and industrial value.

ABBREVIATIONS USED

TLR, Toll-like receptor; TNF-α, tumor necrosis factor-alpha; IL-1β, interleukin-1 beta; NF-κB, nuclear factor-kappa B; MyD88, myeloid differentiation factor 88; LPS, lipopolysaccharide; TRAF6, TNF receptor-associated factor 6; FPLC, fast protein liquid chromatography; LAL, *Limulus* amoebocyte lysate; qPCR, quantitative real-time polymerase chain reaction; EMSA, electrophoretic mobility shift assay; TIRAP, Toll-IL-1 receptor domain-containing adapter protein; FIP, fungal immunomodulatory protein.

Supporting Information Available: Two tables and five figures show the biochemical characteristics of PCP containing p*I* value, amino acid composition, and hemagglutination activity, and testing for endotoxin contamination, IL-1β induction by PCP-incubated TLR2- and TLR4-deficient macrophages, and the activity of PCP after electroelution under native conditions. This material is available free of charge via the Internet at http://pubs.acs.org.

LITERATURE CITED

(1) Mattila, P.; Salo-Vaananen, P.; Konko, K.; Aro, H.; Jalava, T. Basic composition and amino acid contents of mushrooms cultivated in Finland. *J. Agric. Food Chem.* **2002**, *50*, 6419–6422.

(2) Borchers, A. T.; Krishnamurthy, A.; Keen, C. L.; Meyers, F. J.; Gershwin, M. E. The immunobiology of mushrooms. *Exp. Biol. Med. (Maywood)* **2008**, *233*, 259–276.

(3) Yang, N.; Tong, X.; Xiang, Y.; Zhang, Y.; Liang, Y.; Sun, H.; Wang, D. C. Molecular character of the recombinant antitumor lectin from the edible mushroom *Agrocybe aegerita*. *J. Biochem.* **2005**, *138*, 145–150.

(4) Jeurink, P. V.; Noguera, C. L.; Savelkoul, H. F.; Wichers, H. J. Immunomodulatory capacity of fungal proteins on the cytokine production of human peripheral blood mononuclear cells. *Int. Immunopharmacol.* **2008**, *8*, 1124–1133.

(5) Sumisa, F.; Iijima, N.; Ando, A.; Shiga, M.; Kondo, K.; Amano, K.; Nagata, Y. Properties of mycelial aggregate-specific lectin of *Pleurotus cornucopiae* produced in *Pichia pastoris*. *Biosci., Biotechnol., Biochem*. **2004**, *68*, 959–960.
(6) Lin, Y.; Zhang, L.; Chen, L.; Jin, Y.; Zeng, F.; Jin, J.; Wan, B.; Cheung, P. C. Molecular mass and antitumor activities of sulfated derivatives of α-glucan from *Poria cocos* mycelia. *Int. J. Biol. Macromol*. **2004**, *34*, 289–294.
(7) Zhang, G. W.; Liu, H. Y.; Xia, Q. M.; Li, J. Q.; Lu, H.; Zhang, Q. H.; Yao, Z. F. Anti-rejection effect of ethanol extract of *Poria cocos* wolf in rats after cardiac allograft implantation. *Chin. Med. J. (Engl.)* **2004**, *117*, 932–935.
(8) Lin, Z.; Zhu, D.; Yan, Y.; Yu, B. Herbal formula FBD extracts prevented brain injury and inflammation induced by cerebral ischemia-reperfusion. *J. Ethnopharmacol*. **2008**, *118*, 140–147.
(9) Ukiya, M.; Akihisa, T.; Tokuda, H.; Hirano, M.; Oshikubo, M.; Nobukuni, Y.; Kimura, Y.; Tai, T.; Kondo, S.; Nishino, H. Inhibition of tumor-promoting effects by poricoic acids G and H and other lanostane-type triterpenes and cytotoxic activity of poricoic acids A and G from *Poria cocos*. *J. Nat. Prod*. **2002**, *65*, 462–465.
(10) Verstovsek, S.; Maccubbin, D.; Mihich, E. Tumoricidal activation of murine resident peritoneal macrophages by interleukin 2 and tumor necrosis factor α. *Cancer Res*. **1992**, *52*, 3880–3885.
(11) Holler, W.; Goldman, C. K.; Casabo, L.; Nelson, D. L.; Greene, W. C.; Waldmann, T. A. Expression of functional IL-2 receptors by lipopolysaccharide and interferon-γ stimulated human monocytes. *J. Immunol*. **1987**, *138*, 2917–2922.
(12) Keller, R.; Keist, R.; Frei, K. Lymphokines and bacteria, that induce tumoricidal activity, trigger a different secretory response in macrophages. *Eur. J. Immunol*. **1990**, *20*, 695–698.
(13) Takeda, K.; Akira, S. TLR signaling pathways. *Semin. Immunol*. **2004**, *16*, 3–9.
(14) Guha, M.; Mackman, N. LPS induction of gene expression in human monocytes. *Cell. Signal*. **2001**, *13*, 85–94.
(15) Underhill, D. M.; Ozinsky, A.; Smith, K. D.; Aderem, A. Toll-like receptor-2 mediates mycobacteria-induced proinflammatory signaling in macrophages. *Proc. Natl. Acad. Sci. U.S.A*. **1999**, *96*, 14459–14463.
(16) Yoshimura, A.; Lien, E.; Ingalls, R. R.; Tuomanen, E.; Dziarski, R.; Golenbock, D. Cutting edge: recognition of Gram-positive bacterial cell wall components by the innate immune system occurs via Toll-like receptor 2. *J. Immunol*. **1999**, *163*, 1–5.
(17) Hsu, H. Y.; Hua, K. F.; Lin, C. C.; Lin, C. H.; Hsu, J.; Wong, C. H. Extract of Reishi polysaccharides induces cytokine expression via TLR4-modulated protein kinase signaling pathways. *J. Immunol*. **2004**, *173*, 5989–5999.
(18) Lee, J. Y.; Kim, J. Y.; Lee, Y. G.; Rhee, M. H.; Hong, E. K.; Cho, J. Y. Molecular mechanism of macrophage activation by exopolysaccharides from liquid culture of *Lentinus edodes*. *J. Microbiol. Biotechnol*. **2008**, *18*, 355–364.
(19) Hsu, H. C.; Hsu, C. I.; Lin, R. H.; Kao, C. L.; Lin, J. Y. Fip-*vvo*, a new fungal immunomodulatory protein isolated from *Volvariella volvacea*. *Biochem. J*. **1997**, *323*, 557–565.
(20) Zhu, R.; Xu, R.; Jiang, X.; Cai, Y.; Zou, Y.; Du, M.; Qin, L. Expression profile of cancer-related genes in human adult bone marrow-derived neural stemlike cells highlights the need for tumorigenicity study. *J. Neurosci. Res*. **2007**, *85*, 3064–3070.
(21) Tamassia, N.; Le Moigne, V.; Calzetti, F.; Donini, M.; Gasperini, S.; Ear, T.; Cloutier, A.; Martinez, F. O.; Fabbri, M.; Locati, M.; Mantovani, A.; McDonald, P. P.; Cassatella, M. A. The MyD88-independent pathway is not mobilized in human neutrophils stimulated via TLR4. *J. Immunol*. **2007**, *178*, 7344–7356.
(22) Li, H.; Lin, X. Positive and negative signaling components involved in TNFα-induced NF-κB activation. *Cytokine* **2008**, *41*, 1–8.
(23) Medvedev, A. E.; Piao, W.; Shoenfelt, J.; Rhee, S. H.; Chen, H.; Basu, S.; Wahl, L. M.; Fenton, M. J.; Vogel, S. Role of TLR4 tyrosine phosphorylation in signal transduction and endotoxin tolerance. *J. Biol. Chem*. **2007**, *282*, 16042–16053.
(24) Akashi, S.; Shimazu, R.; Ogata, H.; Nagai, Y.; Takeda, K.; Kimoto, M.; Miyake, K. Cutting edge: cell surface expression and lipopolysaccharide signaling via the toll-like receptor 4-MD-2 complex on mouse peritoneal macrophages. *J. Immunol*. **2000**, *164*, 3471–3475.
(25) Wang, Y. Y.; Khoo, K. H.; Chen, S. T.; Lin, C. C.; Wong, C. H.; Lin, C. H. Studies on the immuno-modulating and antitumor activities of *Ganoderma lucidum* (Reishi) polysaccharides:functional and proteomic analyses of a fucose-containing glycoprotein fraction responsible for the activities. *Bioorg. Med. Chem*. **2002**, *10*, 1057–1062.
(26) Kodama, N.; Asakawa, A.; Inui, A.; Masuda, Y.; Nanba, H. Enhancement of cytotoxicity of NK cells by D-fraction, a polysaccharide from *Grifola frondosa*. *Oncol. Rep*. **2005**, *13*, 497–502.
(27) Kino, K.; Yamashita, A.; Yamaoka, K.; Watanabe, J.; Tanaka, S.; Ko, K.; Shimizu, K.; Tsunoo, H. Isolation and characterization of a new immunomodulatory protein, ling zhi-8 (LZ-8), from *Ganoderma lucidium*. *J. Biol. Chem*. **1989**, *264*, 472–478.
(28) Ko, J. L.; Hsu, C. I.; Lin, R. H.; Kao, C. L.; Lin, J. Y. A new fungal immunomodulatory protein, FIP-*fve* isolated from the edible mushroom, *Flammulina velutipes* and its complete amino acid sequence. *Eur. J. Biochem*. **1995**, *228*, 244–249.
(29) Lin, W. H.; Hung, C. H.; Hsu, C. I.; Lin, J. Y. Dimerization of the N-terminal amphipathic α-helix domain of the fungal immunomodulatory protein from *Ganoderma tsugae* (Fip-*gts*) defined by a yeast two-hybrid system and site-directed mutagenesis. *J. Biol. Chem*. **1997**, *272*, 20044–20048.
(30) Kawasaki, K.; Akashi, S.; Shimazu, R.; Yoshida, T.; Miyake, K.; Nishijima, M. Mouse toll-like receptor 4. MD-2 complex mediates lipopolysaccharide-mimetic signal transduction by Taxol. *J. Biol. Chem*. **2000**, *275*, 2251–2254.
(31) Johnson, G. B.; Brunn, G. J.; Kodaira, Y.; Platt, J. L. Receptor-mediated monitoring of tissue well-being via detection of soluble heparan sulfate by Toll-like receptor 4. *J. Immunol*. **2002**, *168*, 5233–5239.
(32) Termeer, C.; Benedix, F.; Sleeman, J.; Fieber, C.; Voith, U.; Ahrens, T.; Miyake, K.; Freudenberg, M.; Galanos, C.; Simon, J. C. Oligosaccharides of hyaluronan activate dendritic cells via Toll-like receptor 4. *J. Exp. Med*. **2002**, *195*, 99–111.
(33) Kasai, H.; He, L. M.; Kawamura, M.; Yang, P. T.; Deng, X. W.; Munkanta, M.; Yamashita, A.; Terunuma, H.; Hirama, M.; Horiuchi, I.; Natori, T.; Koga, T.; Amano, Y.; Yamaguchi, N.; Ito, M. IL-12 production induced by *Agaricus blazei* fraction H (ABH) involves Toll-like receptor (TLR). *Evid. Based Complement. Alternat. Med* **2004**, *1*, 259–267.
(34) Tada, H.; Nemoto, E.; Shimauchi, H.; Watanabe, T.; Mikami, T.; Matsumoto, T.; Ohno, N.; Tamura, H.; Shibata, K.; Akashi, S.; Miyake, K.; Sugawara, S.; Takada, H. *Saccharomyces cerevisiae*- and *Candida albicans*-derived mannan induced production of tumor necrosis factor alpha by human monocytes in a CD14- and Toll-like receptor 4-dependent manner. *Microbiol. Immunol*. **2002**, *46*, 503–512.
(35) Saito, K.; Yajima, T.; Nishimura, H.; Aiba, K.; Ishimitsu, R.; Matsuguchi, T.; Fushimi, T.; Ohshima, Y.; Tsukamoto, Y.; Yoshikai, Y. Soluble branched β-(1,4)glucans from *Acetobacter* species show strong activities to induce interleukin-12 *in vitro* and inhibit T-helper 2 cellular response with immunoglobulin E production *in vivo*. *J. Biol. Chem*. **2003**, *278*, 38571–38578.
(36) Wang, H. W.; Sharp, T. V.; Koumi, A.; Koentges, G.; Boshoff, C. Characterization of an anti-apoptotic glycoprotein encoded by Kaposi's sarcoma-associated herpes virus which resembles a spliced variant of human survivin. *EMBO J*. **2002**, *21*, 2602–2615.
(37) Pietrella, D.; Bistoni, G.; Corbucci, C.; Perito, S.; Vecchiarelli, A. *Candida albicans* mannoprotein influences the biological function of dendritic cells. *Cell. Microbiol*. **2006**, *8*, 602–612.
(38) Pietrella, D.; Lupo, P.; Rachini, A.; Sandini, S.; Ciervo, A.; Perito, S.; Bistoni, F.; Vecchiarelli, A. A *Candida albicans* mannoprotein deprived of its mannan moiety is efficiently taken up and processed by human dendritic cells and induces T-cell activation without stimulating proinflammatory cytokine production. *Infect. Immun*. **2008**, *76*, 4359–4367.

Received April 6, 2009. Revised manuscript received June 11, 2009. Accepted June 14, 2009. This work was supported by a grant (96-2313-B-002-047-MY3) from the National Science Council of Taiwan.